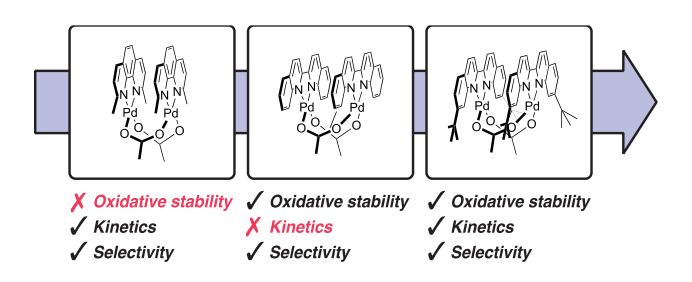
# Mechanism-guided design of robust palladium catalysts for selective aerobic oxidation of polyols

Summer Ramsay-Burrough,<sup>a</sup> Daniel P. Marron,<sup>a</sup> Keith C. Armstrong,<sup>a</sup> Trevor J. Del Castillo,<sup>a</sup> Richard N. Zare,<sup>a</sup> and Robert M. Waymouth<sup>a,\*</sup>

<sup>a</sup>Department of Chemistry, Stanford University, Stanford, California 94305, United States \*waymouth@stanford.edu

#### Abstract

The palladium complex  $[(L_1)]Pd(\mu-OAc)]_2[OTf]_2(L_1 = neocuproine)$  is a selective catalyst for the aerobic oxidation of vicinal polyols to α-hydroxyketones, but competitive oxidation of the ligand methyl groups limits turnover number and necessitates high Pd loadings. Replacement of the neocuproine ligand with 2,2'-biquinoline ligands was investigated as a strategy to improve catalyst performance and explore the relationship between ligand structure and reactivity. Evaluation of  $[(L_2)]Pd(\mu-OAc)]_2[OTf]_2(L_2 = 2,2'-biquinoline)$  as a catalyst for aerobic alcohol oxidation revealed a threefold enhancement in turnover number relative to the neocuproine congener, but a much slower rate. Mechanistic studies indicated that the slow rates observed with L2 were a consequence of precipitation of an insoluble trinuclear palladium species — (L<sub>2</sub>Pd)<sub>3</sub>(µ-O)<sub>2</sub><sup>2+</sup> formed during catalysis and characterized by high-resolution electrospray ionization mass spectrometry. Density functional theory was used to predict that a sterically modified biguinoline ligand,  $L_3 = 7.7$ '-di-tert-butyl-2,2'-biquinoline, would disfavor the formation of the trinuclear  $(LPd)_3(\mu-O)_2^{2+}$  species. This design strategy was validated, as catalytic aerobic oxidation with [(L<sub>3</sub>)]Pd(μ-OAc)]<sub>2</sub>[OTf]<sub>2</sub> is both robust and rapid, marrying the kinetics of the parent L<sub>1</sub>-supported system with the high aerobic turnover numbers of the L<sub>2</sub>-supported system. Changes in ligand structure were also found to modulate regioselectivity in the oxidation of complex glycoside substrates, providing new insights into structure-selectivity relationships with this class of catalysts.



## Introduction

Chemoselective catalytic oxidation of alcohols <sup>1-11</sup> is a powerful strategy for the sustainable production of fine and commodity chemicals with minimal time, waste, and cost. <sup>12-14</sup> Air is a convenient and attractive terminal oxidant, but partially reduced oxygen can generate highly active species that participate in competitive, nonselective reactions. <sup>15-16</sup> We previously reported that the dimeric cationic palladium complex  $[(\mathbf{L}_1)\text{Pd}(\mu\text{-OAc})]_2[\text{OTf}]_2$  ( $\mathbf{L}_1$  = neocuproine = 2,9-dimethyl-1,10-phenanthroline) is an effective catalyst precursor for the oxidation of vicinal polyols under mild conditions to afford  $\alpha$ -hydroxyketones with high regio- and chemoselectivities. <sup>17-24</sup> This catalyst is also selective for the direct oxidation of carbohydrates to 3-ketoses, <sup>23, 25-29</sup> a complex transformation that typically demands multiple steps of protection/deprotection. <sup>30-31</sup> However, under aerobic conditions, H atom abstraction and subsequent oxidation of the benzylic methyl C-H bonds on the neocuproine ligand generates inactive palladium carboxylate species (Figure 1A, species **1\*\***). <sup>17, 21, 24</sup> This competitive ligand oxidation limits catalyst lifetime and necessitates high palladium loadings to achieve high conversions.

#### A. Proposed catalytic cycle for alcohol oxidation with $[(L_1)Pd(\mu-OAc)]_2[OTf]_2$

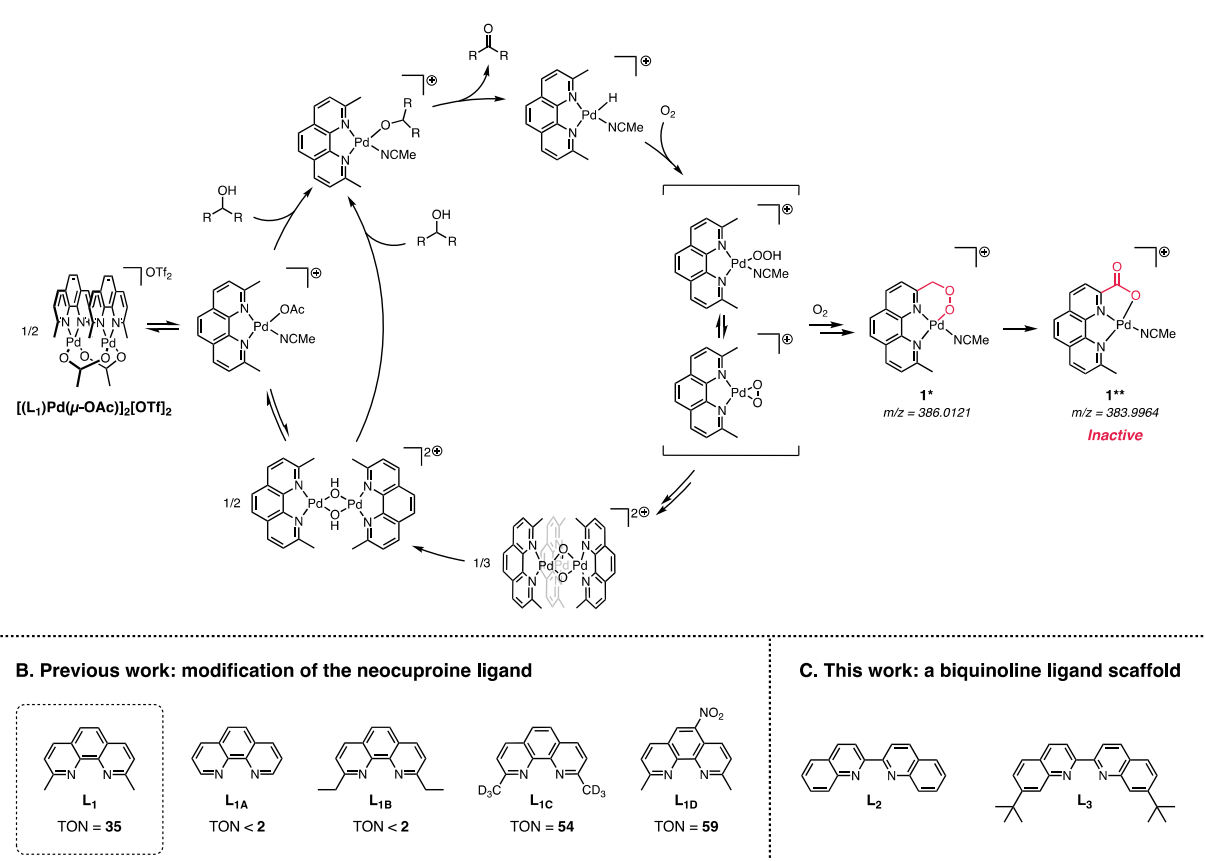


**Figure 1. A:** Proposed catalytic cycle for alcohol oxidation with  $[(L_1)Pd(\mu-OAc)]_2[OTf]_2$ . **B:** Previously studied phenanthroline-based ligands and the performance of corresponding  $[(L)Pd(\mu-OAc)]_2[OTf]_2$  complexes as catalysts for aerobic oxidation of 1,2-propanediol (reaction conditions: 0.5 mol % Pd, 0.25 M 1,2-propanediol in CH<sub>3</sub>CN, rt, 24 hr). <sup>24</sup> **C:** Ligands evaluated in this work;  $L_2 = 2,2$ '-biquinoline and  $L_3 = 7,7$ '-di-tert-butyl-2,2'-biquinoline.

Previous work demonstrated modest improvements in catalyst lifetime by introducing electron-withdrawing substituents onto the neocuproine scaffold<sup>24</sup> or by deuterating the 2,9-methyl groups to reduce the rate of ligand oxidation (Figure 1B,  $L_{1C}$  and  $L_{1D}$ ). <sup>19, 24, 32</sup> More significant

improvements were achieved by the addition of sacrificial H atom donors such as phenols to reaction mixtures, <sup>23-24</sup> but these strategies can complicate product isolation.

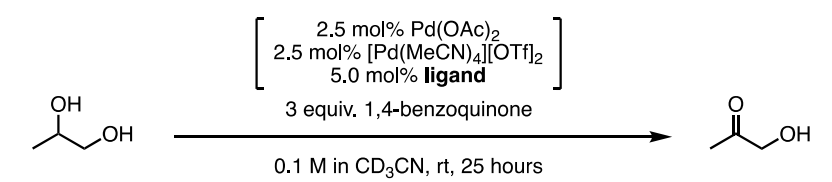
While the methyl substituents at the 2 and 9 positions of the neocuproine ligand are an oxidative liability, substituents at these positions are necessary for catalysis. The neocuproine-ligated Pd complex  $[(L_1)Pd(\mu\text{-OAc})]_2[OTf]_2$  exhibits fast initial rates of alcohol oxidation, <sup>19, 24</sup> but the phenanthroline-ligated complex  $[(\text{phenanthroline})Pd(\mu\text{-OAc})]_2[OTf]_2$  is inactive at room temperature as a consequence of the formation of the stable and inactive species  $[(\text{phenanthroline})Pd(\mu\text{-OH})]_2[OTf]_2^{1, 19, 33}$  under catalytic conditions (Figure 1B,  $L_{1A}$ ). However, the 2,9-diethyl-1,10-phenanthroline complex (Figure 1B,  $L_{1B}$ ) is also inactive at room temperature. <sup>24</sup> The remarkable sensitivity of catalytic performance to ligand steric effects has compromised previous efforts to modify  $[(L)Pd(\mu\text{-OAc})]_2[OTf]_2$  complexes <sup>19, 24, 32</sup> to improve oxidative stability and maintain high rates at room temperature.

Herein we describe the mechanism-guided design of biquinoline-supported  $^{34-35}$  catalysts  $[(L_2)Pd(\mu\text{-OAc})]_2[OTf]_2$  ( $L_2$  = 2,2'-biquinoline) and  $[(L_3)Pd(\mu\text{-OAc})]_2[OTf]_2$  ( $L_3$  = 7,7'-di-tert-butyl-2,2'-biquinoline) for selective alcohol oxidation (Figure 1C). These biquinoline-type ligands lack the benzylic C-H bonds that are susceptible to oxidation in the parent neocuproine-ligated system; as a consequence, they are more robust under aerobic conditions. Catalysts derived from the biquinoline ligands  $L_2$  and  $L_3$  also exhibit high chemoselectivity, enabling access to valuable chemical products with low loadings of palladium and operationally simple conditions.

#### **Results and Discussion**

# Chemoselective oxidation of 1,2-propanediol with [(L<sub>2</sub>)Pd(µ-OAc)]<sub>2</sub>[OTf]<sub>2</sub>

To evaluate the effectiveness of different chelating ligands for the oxidation of 1,2-propanediol, a model vicinal diol substrate,  $[(L)Pd(\mu-OAc)]_2[OTf]_2$  complexes were generated *in situ*<sup>24</sup> and evaluated using 1,4-benzoquinone as a terminal oxidant under anaerobic conditions (Figure 2). With the ligand 2,2'-biquinoline ( $L_2$ ), 94% conversion of 1,2-propanediol was observed by NMR after 25 hours. As observed with the neocuproine-ligated congener,<sup>20, 24</sup>  $[(L_2)Pd(\mu-OAc)]_2[OTf]_2$  exhibits high chemoselectivity for oxidation of only the secondary alcohol in the vicinal diol, giving an 86% yield of hydroxyacetone as determined by NMR (91% selectivity<sup>36</sup>). Under the same conditions the reaction with the neocuproine ligand  $L_1$  provided a comparable yield of hydroxyacetone, whereas reactions with 2,2'-bipyridine and 1,10-phenanthroline ligands were ineffective and produced minimal hydroxyacetone. Similar results with *in situ* generated  $L_1$ - and  $L_2$ -supported catalysts were also achieved using only a slight excess (1.2 equivalents) of 1,4-benzoquinone (TONs of 19 and 18, respectively).



Ligand	% yield (NMR)	TON
L = neocuproine (L <sub>1</sub> )	89	18
$L = 2,2$ '-biquinoline ( $L_2$ )	86	17
L = 2,2'-bipyridine	3	<2
L = 1,10-phenanthroline	7	<2
L = none	15	3

**Figure 2.** Anaerobic oxidation of 1,2-propanediol with [(L)Pd( $\mu$ -OAc)]<sub>2</sub>[OTf]<sub>2</sub> (formed *in situ*) and 1,4-benzoquinone as a terminal oxidant. Yields were determined by <sup>1</sup>H NMR; TON is calculated as %yield hydroxyacetone/mol% Pd.

As we had anticipated that complexes supported by the biquinoline ligand  $L_2$  would be more robust to oxidative degradation than those supported by  $L_1$ , we evaluated the activity of  $[(L_2)Pd(\mu-OAc)]_2[OTf]_2$  using air as a terminal oxidant. Catalysts supported by  $L_1$  and  $L_2$  were formulated *in situ* and tested for the oxidation of 1,2-propanediol in ambient air (Figure 3, Table S1). Under these conditions, catalysis with the biquinoline-ligated  $[(L_2)Pd(\mu-OAc)]_2[OTf]_2$  afforded hydroxyacetone with higher turnover numbers (TONs) than catalysis with the neocuproine-ligated complex.

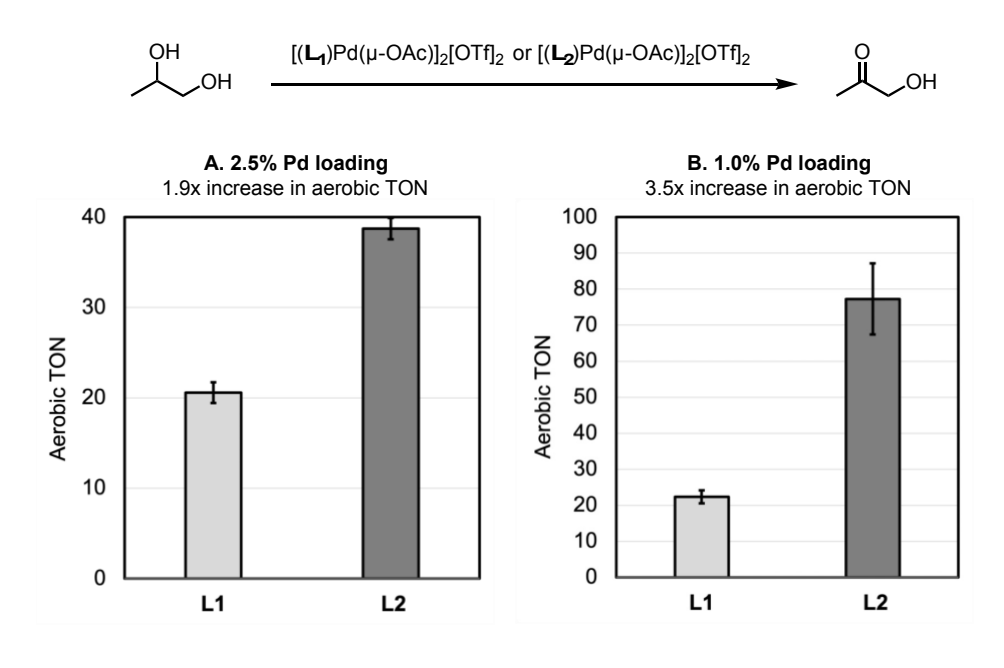


**Figure 3.** TONs for the aerobic oxidation of 1,2-propanediol in the presence of  $[(L_1)Pd(\mu-OAc)]_2[OTf]_2$  and  $[(L_2)Pd(\mu-OAc)]_2[OTf]_2$  (both catalysts prepared *in situ* as described in Figure 2). **A**: 2.5 mol% Pd, 0.1 M 1,2-propanediol in CD<sub>3</sub>CN, 45°C, 48 hr. **B**: 1.0 mol% Pd, 0.1 M 1,2-propanediol in CD<sub>3</sub>CN, 45°C, 192 hr. Yields were determined by <sup>1</sup>H NMR. TON is calculated as %yield hydroxyacetone/mol% Pd. TON values are an average of three sets of duplicate experiments (total n=6); error bars represent +/- 1 standard deviation.

At 2.5 mol% Pd loading, reactions catalyzed by  $[(L_2)Pd(\mu\text{-OAc})]_2[OTf]_2$  generated hydroxyacetone in 97% yield (TON = 39) after 48 hours. By comparison, the yield of hydroxyacetone in the same timeframe with  $[(L_1)Pd(\mu\text{-OAc})]_2[OTf]_2$  was 52% (TON = 21), roughly half of that observed with  $L_2$  (Figure 3A). At 1.0 mol% Pd loading, the difference in TON between  $L_1$  and  $L_2$  was more pronounced: complexes bearing  $L_2$  afforded hydroxyacetone in 77% yield (TON = 77), whereas the yield of hydroxyacetone from complexes bearing  $L_1$  was only 22% (TON = 22), demonstrating a greater than threefold increase in aerobic TON with  $L_2$  (Figure 3B). These results imply that the biquinoline ligand is more oxidatively robust than the neocuproine ligand. However,  $[(L_2)Pd(\mu\text{-OAc})]_2[OTf]_2$  exhibited very slow rates for the aerobic oxidation of 1,2-propanediol: at 1.0 mol% Pd loadings, high conversions required 8 days of reaction time. Thus, the performance advantages of the more oxidatively robust biquinoline ligand are mitigated by the slow reaction kinetics.

In an attempt to improve reaction rates with biquinoline-type ligands, we investigated electronically modulated variants of the biquinoline ligand  $L_2$ . An electron-rich ligand L=6,6'-dimethoxy-2,2'-biquinoline and an electron-poor ligand L=6,6'-bis(trifluoromethyl)-2,2'-biquinoline were synthesized and tested for the oxidation of 1,2-propanediol. However, neither of these variants provided a meaningful improvement in rate relative to the unfunctionalized biquinoline ligand.

#### Investigation of Pd speciation in reaction mixtures by HR-MS

During the course of investigation of  $[(L_2)Pd(\mu-OAc)]_2[OTf]_2$  we consistently observed orange-yellow precipitate in reaction mixtures (Figure S16). We suspected that precipitation of Pd-containing species might be decreasing the effective Pd concentration in solution, with a deleterious effect on reaction rate. To test this hypothesis, the supernatant of the reaction mixture was drawn off and a portion of the remaining solid was removed, taken up in acetonitrile, and analyzed by high-resolution electrospray ionization mass spectrometry (ESI-MS).<sup>22, 37-38</sup> Despite the poor solubility of the solid material, the high sensitivity of ESI-MS provided adequate signal to identify  $(L_2Pd)_3(\mu-O)_2^{2+}$  (m/z=560.0014) as the major Pd species (Figures 4A and 4C, Figure S26). Analogous trinuclear  $\mu$ -oxo Pd species have been observed in previous studies of the neocuproine-supported catalyst (Figure 1).<sup>21-22</sup>

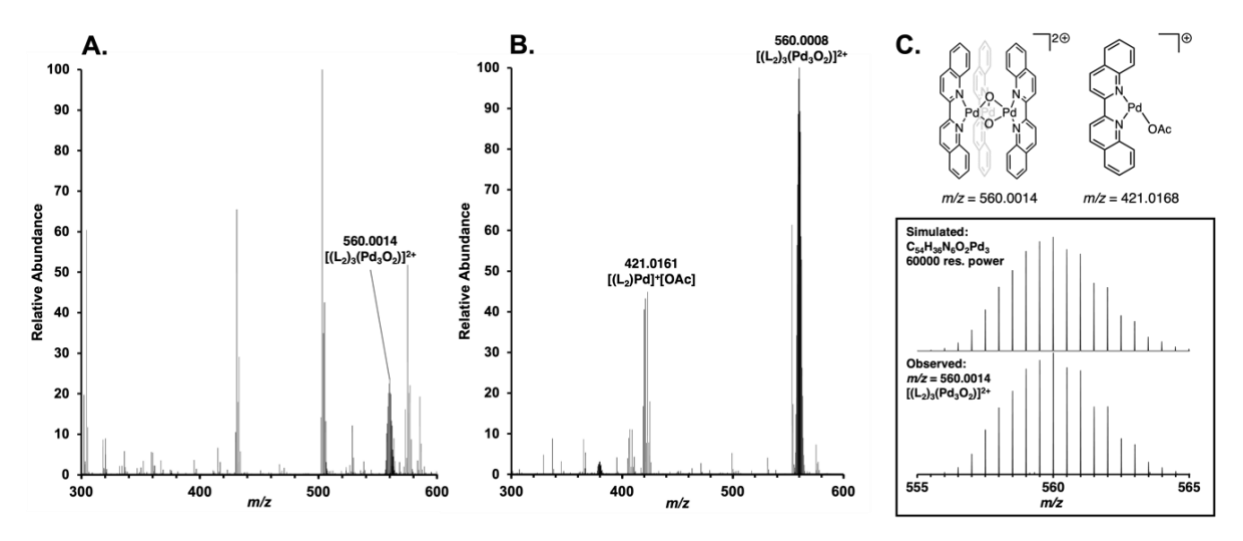


**Figure 4. A:** Mass spectrum of precipitate from a catalytic reaction containing  $[(L_2)Pd(\mu-OAc)]_2[OTf]_2$ . **B:** Mass spectrum of aerobic oxidation of 1,2-propanediol catalyzed by  $[(L_2)Pd(\mu-OAc)]_2[OTf]_2$  (2.5 mol % Pd, 0.1 M 1,2-propanediol in CH<sub>3</sub>CN, 45°C, 15 minutes). **C:** Chemical structures of ions observed in **A** and **B**. Peaks containing palladium above 10% relative abundance are labeled and identified.

To further investigate the speciation of Pd in catalytic aerobic oxidation reaction mixtures, we employed high-resolution ESI-MS to monitor the aerobic oxidation of 1,2-propanediol with  $[(L_2)Pd(\mu-OAc)]_2[OTf]_2$  (generated *in situ*, 2.5 mol% Pd, 45°C, 0.1 M substrate in CH<sub>3</sub>CN) over the course of multiple hours. The dicationic tripalladium species  $(L_2Pd)_3(\mu-O)_2^{2+}$  (m/z = 560.0014) was observed as early as 5 minutes (Figure S32). By the 15-minute timepoint other Pd-containing peaks in the spectrum corresponded to  $(L_2)Pd(OAc)^+$  (m/z = 421.0168) and  $[(L_2)Pd(\mu-OH)]_2^{2+}$  (m/z = 380.0059) (Figures 4B and 4C, Figure S33). After 15 minutes, 1 hour, and 5 hours of reaction time,  $(L_2Pd)_3(\mu-O)_2^{2+}$  remained the major Pd species detected by ESI-MS in the reaction mixture.

To confirm the identity of this species and allow for further studies of its reactivity,  $[(\mathbf{L_2}Pd)_3(\mu-O)_2][OTf]_2$  was independently synthesized.  $[(\mathbf{L_2}Pd)_3(\mu-O)_2][OTf]_2$  forms rapidly as an orange-yellow solid upon addition of excess  $H_2O_2$  to an acetonitrile solution of  $[(\mathbf{L_2})Pd(\mu-OAc)]_2[OTf]_2$ . The product  $[(\mathbf{L_2}Pd)_3(\mu-O)_2][OTf]_2$  (sparingly soluble in CH<sub>3</sub>CN and DMSO) was fully characterized by <sup>1</sup>H NMR, <sup>13</sup>C NMR, <sup>19</sup>F NMR, high-resolution ESI-MS, and elemental analysis.

To determine the catalytic and/or kinetic competence of the trinuclear complex  $[(\mathbf{L}_2Pd)_3(\mu-O)_2][OTf]_2$  for alcohol oxidation, 0.1 mmol 1,2-propanediol was subjected to oxidation using 0.005 mmol  $[(\mathbf{L}_2Pd)_3(\mu-O)_2][OTf]_2$  as a catalyst (15 mol% Pd, 0.1 M substrate in CD<sub>3</sub>CN, 45°C) and monitored by NMR. Even at these high Pd loadings, less than 30% conversion (TON = 2) of the propanediol substrate was observed after 48 hours. Analysis of a related reaction mixture (0.1 mmol 1,2-propanediol, 0.00167 mmol  $[(\mathbf{L}_2Pd)_3(\mu-O)_2][OTf]_2$ , 5 mol% Pd, 45°C, 0.1 M substrate in CH<sub>3</sub>CN) by ESI-MS revealed  $(\mathbf{L}_2Pd)_3(\mu-O)_2^{2+}$  as the only major Pd-containing ion (Figure S27). These data are consistent with the hypothesis that formation and precipitation of the insoluble  $[(\mathbf{L}_2Pd)_3(\mu-O)_2][OTf]_2$  during the course of a reaction is responsible for the low rates observed in the presence of the biquinoline-ligated  $[(\mathbf{L}_2)Pd(\mu-OAc)]_2[OTf]_2$ .

The trinuclear  $[(L_2Pd)_3(\mu-O)_2][OTf]_2$  is an inefficient catalyst precursor on its own, but some catalytic activity can be recovered by the addition of  $[Pd(MeCN)_4][OTf]_2$ . When 0.0025 mmol  $[(L_2Pd)_3(\mu-O)_2][OTf]_2$  was combined with 0.0025 mmol  $[Pd(MeCN)_4][OTf]_2$  (10 mol% Pd, 45°C, 0.1 M substrate in CD<sub>3</sub>CN), the oxidation of 0.1 mmol 1,2-propanediol proceeded to >98% conversion after 48 hours. A comparable reaction mixture (0.1 mmol 1,2-propanediol, 0.00167 mmol

[( $L_2$ Pd)<sub>3</sub>(μ-O)<sub>2</sub>][OTf]<sub>2</sub>, 0.00167 mmol [Pd(MeCN)<sub>4</sub>][OTf]<sub>2</sub>, 6.7 mol% Pd, 45°C, 0.1 M substrate in CH<sub>3</sub>CN) was monitored by ESI-MS; though the major ion observed was m/z = 560.0014, corresponding to ( $L_2$ Pd)<sub>3</sub>(μ-O)<sub>2</sub><sup>2+</sup>, a number of additional Pd-containing ions — including [( $L_2$ )Pd(Cl)(MeCN)]<sup>+</sup> (m/z = 437.9989) and [( $L_2$ )Pd(μ-OH)]<sub>2</sub><sup>2+</sup> (m/z = 380.0059) — were also observed in the reaction mixture (Figure S28). These results demonstrate that [( $L_2$ Pd)<sub>3</sub>(μ-O)<sub>2</sub>][OTf]<sub>2</sub> can react with the additional [Pd(MeCN)<sub>4</sub>][OTf]<sub>2</sub> to regenerate some active catalyst species, as was observed in similar studies with the neocuproine congener [( $L_1$ Pd)<sub>3</sub>(μ-O)<sub>2</sub>][BF<sub>4</sub>]<sub>2</sub>.<sup>21</sup>

Despite the slow rates observed for aerobic alcohol oxidation with the biquinoline complex [(L<sub>2</sub>)Pd(u-OAc)]<sub>2</sub>[OTf]<sub>2</sub>, the higher TONs observed (Figure 3) suggest that this complex is more oxidatively robust than the corresponding neocuproine complex  $[(L_1)Pd(\mu-OAc)]_2[OTf]_2$ . To further test this hypothesis, the speciation of Pd complexes during the course of aerobic oxidation of 1,2propanediol with in situ generated  $[(L_1)Pd(\mu-OAc)]_2[OTf]_2$  and  $[(L_2)Pd(\mu-OAc)]_2[OTf]_2$  was monitored to identify oxidized catalyst species. As previously reported, oxidation of 1,2propanediol under aerobic conditions with the neocuproine complex  $[(L_1)Pd(\mu-OAc)]_2[OTf]_2$  is accompanied by rapid ligand oxidation. 17, 19, 21 When these reactions were monitored by ESI-MS, ions corresponding to ligand oxidation (e.g. m/z = 386.0121, Figure 1) were observed as early as 5 minutes of reaction time (Figure S29). In contrast, for analogous reactions with the biquinoline complex  $[(L_2)Pd(\mu-OAc)]_2[OTf]_2$ , ions associated with ligand oxidation (e.g. m/z = 418.0172, Figure 5 and Figure S34) were only evident after multiple (>5) hours of reaction time. Though these data indicate that oxidation of the biguinoline ligand can occur, the high conversions of propanediol achieved with  $[(L_2)Pd(\mu-OAc)]_2[OTf]_2$  suggest that it is unlikely that ligand oxidation is a major pathway of catalyst deactivation. The continued activity of  $[(\mathbf{L}_2)Pd(\mu-OAc)]_2[OTf]_2$  over the course of many days under aerobic conditions supports this conclusion.

**Figure 5.** Proposed catalytic cycle for alcohol oxidation with  $[(L_2)Pd(\mu\text{-OAc})]_2[OTf]_2$ , highlighting Pd species hypothesized to be associated with slow catalysis.

These data and observations indicate that during the course of catalytic reactions with  $[(\mathbf{L}_2)Pd(\mu-OAc)]_2[OTf]_2$ , a significant fraction of Pd is sequestered as the insoluble trimeric species  $(\mathbf{L}_2Pd)_3(\mu-O)_2^{2+}$  (Figure 5). ESI-MS of catalytic mixtures shows that this species is abundant throughout catalysis, and NMR experiments show that while this species is catalytically competent, it is slow to re-enter the catalytic cycle. The sequestration of Pd as this insoluble multinuclear species limits the concentration of active catalyst in solution, offering an explanation for the relatively low observed rates with  $[(\mathbf{L}_2)Pd(\mu-OAc)]_2[OTf]_2$ .

# Computationally guided selection of a second-generation biquinoline ligand, L<sub>3</sub>

DFT calculations were used to identify modified biquinoline ligands that might retain the oxidative stability of the biquinoline ligand  $L_2$  but disfavor association to multi-palladium species such as  $(LPd)_3(\mu-O)_2^{2^+}$ . For these studies, we evaluated the energetics of isodesmic ligand exchange between a symmetrically di-substituted biquinoline ligand  $L_X$  and the trinuclear neocuproine complex  $(L_1Pd)_3(\mu-O)_2^{2^+}$  to yield  $L_1$  and  $(L_XPd)_3(\mu-O)_2^{2^+}$  (Figure 6, Table S7). We reasoned that if this forward reaction is thermodynamically unfavorable for a ligand  $L_X$ , then  $(L_XPd)_3(\mu-O)_2^{2^+}$  would be less likely to speciate during catalysis. All computations were performed using the Gaussian 16 software package<sup>39</sup> with the B3LYP DFT functional<sup>40-41</sup> and the 6-31G\* basis set<sup>42-44</sup> for light atoms and the LANL2DZ ECP basis<sup>45</sup> for Pd atoms.

L <sub>x</sub>	L <sub>x</sub> substitution		∆G (kcal/mol) in CH₃ <b>CN</b>
L <sub>2</sub>	R <sub>1</sub> = H	$R_2 = H$	+ 1.0
L <sub>3</sub>	$R_1 = C(CH_3)_3$	$R_2 = H$	+ 42
L <sub>4</sub>	$R_1 = CH_3$	$R_2 = H$	+ 10
L <sub>5</sub>	R <sub>1</sub> = H	$R_2 = C(CH_3)_3$	Could not be determined
L <sub>6</sub>	R <sub>1</sub> = H	$R_2 = CH_3$	+ 56

**Figure 6.** Scheme of isodesmic ligand exchange between  $L_X$  and  $L_1$  (top) and  $\Delta G$  in CH<sub>3</sub>CN of the forward reaction for each  $L_X$  (bottom).  $\Delta G$  values were calculated from free energy values extracted from DFT frequency calculations on optimized structures (B3LYP/6-31G\*/ LANL2DZ, SMD solvent model).

The isodesmic ligand exchange between the unfunctionalized biquinoline ligand  $L_2$  ( $R_1 = H$ ,  $R_2 = H$ ) and  $(L_1Pd)_3(\mu-O)_2^{2+}$  is effectively thermoneutral: the formation of  $(L_2Pd)_3(\mu-O)_2^{2+}$  is calculated to be endergonic by only 1.0 kcal/mol in CH<sub>3</sub>CN (SMD solvent model) and 0.2 kcal/mol in the gas phase (Table S6). However, ligand exchanges to form  $(L_xPd)_3(\mu-O)_2^{2+}$  with sterically hindered 7-and 8-disubstituted biquinoline ligands  $(L_3-L_6)$  were calculated to be endergonic. For the sterically-demanding  $L_3$  ( $R_1 = C(CH_3)_3$ ,  $R_2 = H$ ),  $\Delta G$  was calculated to be +42 kcal/mol in CH<sub>3</sub>CN. For the less bulky methyl congener  $L_4$  ( $R_1 = CH_3$ ,  $R_2 = H$ ),  $\Delta G$  was calculated to be +10 kcal/mol in CH<sub>3</sub>CN. Isodesmic ligand exchanges with biquinoline ligands functionalized at the 8-position ( $L_5$ 

and  $L_6$ ) were calculated to be highly endergonic; for  $L_5$  (R<sub>1</sub> = H, R<sub>2</sub> = C(CH<sub>3</sub>)<sub>3</sub>,), geometry optimization of  $(L_5\text{Pd})_3(\mu\text{-O})_2^{2^+}$  did not converge, suggesting an unstable trimeric structure with this ligand.

We hypothesized that if formation of  $(L_2Pd)_3(\mu-O)_2^{2+}$  is a major contributing factor to slow reaction rates with the  $L_2$ -supported catalyst, then the use of a more sterically demanding ligand might yield a catalyst with more favorable reaction kinetics. Based on the results of the DFT calculations we chose to synthesize 7,7'-di-tert-butyl-2,2'-biquinoline  $(L_3)$  because of the high computed thermodynamic barrier to formation of  $(L_3Pd)_3(\mu-O)_2^{2+}$ , the absence of benzylic  $C(sp^3)$ -H bonds on the ligand, and the anticipated higher solubility of complexes ligated by  $L_3$ .

# Evaluation of [(L<sub>3</sub>)Pd(μ-OAc)]<sub>2</sub>[OTf]<sub>2</sub> for aerobic oxidation of 1,2-propanediol

 $L_3$  was synthesized from 3-tert-butylaniline via formation of 7-tert-butylquinoline, which was oxidized to form the quinoline N-oxide, coupled, and reduced to yield 7,7'-di-tert-butyl-2,2'-biquinoline.<sup>46</sup> The complex  $[(L_3)Pd(\mu-OAc)]_2[OTf]_2$  was synthesized via the comproportionation-type reaction of  $L_3Pd(OAc)_2$  and  $[L_3Pd(CH_3CN)_4][OTf]_2$  (Figure 7).

Figure 7. Synthesis of [(L<sub>3</sub>)Pd(μ-OAc)]<sub>2</sub>[OTf]<sub>2</sub>.

The activity of  $[(L_3)Pd(\mu-OAc)]_2[OTf]_2$  was then compared to that of the neocuproine complex  $[(L_1)Pd(\mu-OAc)]_2[OTf]_2$  for the aerobic oxidation of 1,2-propanediol at low Pd loadings. At 2.5 mol% Pd loadings, oxidation using the  $L_3$ -supported catalyst reached 93% conversion within 1 hour and >99% conversion in 3 hours (Figure 8A) and retained the high selectivity for secondary alcohol oxidation in vicinal diols, with a 90% yield of hydroxyacetone in 3 hours by NMR. The reaction performed in parallel with the  $L_1$ -supported catalyst reached 58% conversion in the first hour of reaction but did not proceed to completion within 18 hours.

The improved oxidative stability of  $[(L_3)Pd(\mu\text{-OAc})]_2[OTf]_2$  became apparent upon reduction of the Pd loading to 1.0 mol% (Figure 8B). The oxidation of 1,2-propanediol proceeds to 90% conversion with an 81% yield of hydroxyacetone by NMR after 18 hours. This translates to an aerobic TON of 81 — comparable to the TONs of 75-85 observed with  $L_2$  at the same catalyst loading, but achieved overnight rather than over the course of a week. More resolved comparison of initial rates revealed that  $[(L_3)Pd(\mu\text{-OAc})]_2[OTf]_2$  is slightly faster than  $[(L_1)Pd(\mu\text{-OAc})]_2[OTf]_2$  under these conditions (Figure S18). These initial results demonstrated that catalysis with  $L_3$  represents a marriage of the best qualities of the neocuproine ligand  $L_1$  and the biquinoline ligand  $L_2$  — rapid reactivity and oxidative stability, respectively.

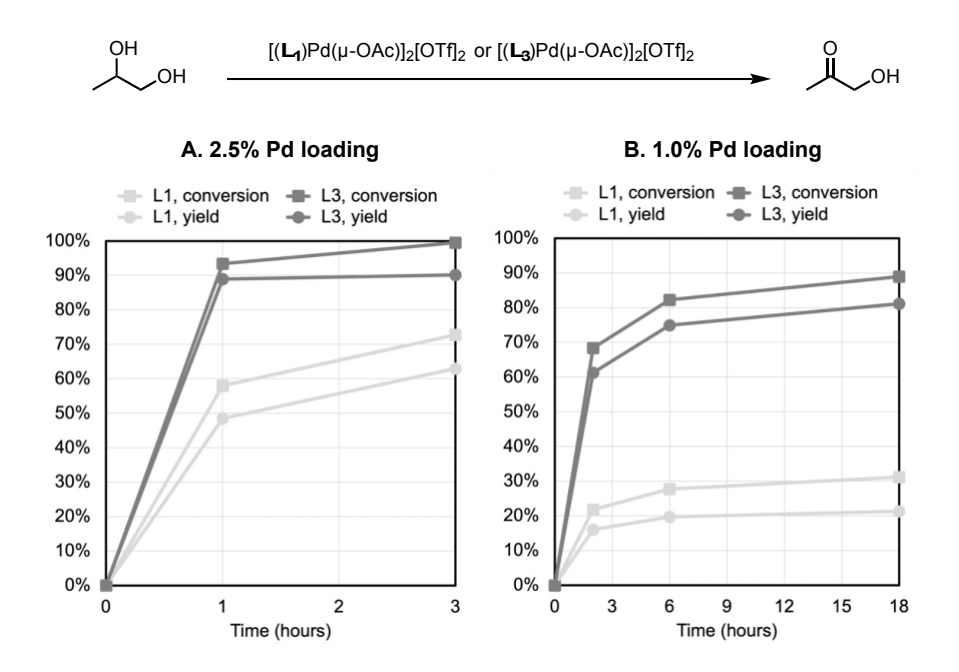


**Figure 8.** Reaction monitoring of the oxidation of 1,2-propanediol in the presence of  $[(L_1)Pd(\mu-OAc)]_2[OTf]_2$  and  $[(L_3)Pd(\mu-OAc)]_2[OTf]_2$ . **A:** 2.5 mol% Pd, 0.1 M 1,2-propanediol in CD<sub>3</sub>CN, 45°C. **B:** 1.0 mol% Pd, 0.1 M 1,2-propanediol in CD<sub>3</sub>CN, 45°C. Conversions and yields were determined by <sup>1</sup>H NMR.

High-resolution ESI-MS was used to gain insight into the speciation of Pd under typical conditions for catalysis with  $[(L_3)Pd(\mu\text{-OAc})]_2[OTf]_2$ . An aerobic oxidation reaction mixture of 1,2-propanediol with *in situ* generated  $[(L_3)Pd(\mu\text{-OAc})]_2[OTf]_2$  (2.5 mol% Pd, 45°C, 0.1 M in CH<sub>3</sub>CN) was sampled at various time points. At early time points, the broad isotopic envelope centered at m/z = 727.6885 corresponding to the  $(L_3Pd)_3(\mu\text{-O})_2^{2^+}$  ion was detectable (Figure S35), but at very low relative abundance (less than 10%). At longer reaction times (1 hour and 24 hours), this ion was conspicuously absent (Figure S37). These data indicate that formation of multi-Pd species is still possible with  $L_3$  despite its increased steric bulk. Overall, however, the speciation of  $[(L_3)Pd(\mu\text{-OAc})]_2[OTf]_2$  as observed by mass spectrometry indicates that formation of  $(L_3Pd)_3(\mu\text{-O})_2^{2^+}$  is disfavored relative to the  $L_2$  system.

ESI-MS spectra taken after addition of 1000 equivalents of  $H_2O_2$  to a solution of  $[(L_3)Pd(\mu-OAc)]_2[OTf]_2$  in  $CH_3CN$  did not show any peaks attributable to  $(L_3Pd)_3(\mu-O)_2^{2^+}$  (Figure S38). The improved catalytic performance of  $[(L_3)Pd(\mu-OAc)]_2[OTf]_2$ , in combination with the minimal amount of  $(L_3Pd)_3(\mu-O)_2^{2^+}$  observed over the course of multiple ESI-MS experiments, suggests that the higher activity observed with the substituted biquinoline  $L_3$  compared to the unfunctionalized biquinoline  $L_2$  is at least partially attributable to the increased steric demand of the ligand, which disfavors the formation of multi-palladium species like  $(L_3Pd)_3(\mu-O)_2^{2^+}$ . This is consistent with the conclusions drawn from the computational isodesmic ligand exchange detailed above (Figure 6), which indicate that the addition of steric bulk to functionalized biquinoline ligands  $L_X$  disfavors the formation of  $(L_XPd)_3(\mu-O)_2^{2^+}$ .

## X-ray crystallography

Single crystals of  $[(\mathbf{L}_2)Pd(\mu\text{-OAc})]_2[OTf]_2$  and  $[(\mathbf{L}_3)Pd(\mu\text{-OAc})]_2[OTf]_2$  suitable for X-ray diffraction were grown by diffusion of diethyl ether into solutions of the respective complexes in acetonitrile.

Crystal structures of the  $L_{2^-}$  and  $L_{3^-}$ supported catalysts are shown in Figure 9 alongside a reproduction of the previously reported crystal structure of  $[(L_1)Pd(\mu-OAc)]_2[OTf]_2$ . All three ligands yield similar acetate-bridged dimeric complexes, but slight variations are observed as a function of the different ligand structures.

Crystals of  $[(L_2)Pd(\mu-OAc)]_2[OTf]_2$  contain two subtly distinct dimers in the unit cell (Figure S23, Figure S24). The C-C-C torsion angles (representing the torsion between the two quinoline halves of the ligand) of the four ligands in the two dimers in the unit cell are 8.95°, 1.59° | 1.49°, 8.34°. For comparison, the corresponding torsion angles obtained from the previously reported crystal structure of  $[(L_1)Pd(\mu-OAc)]_2[OTf]_2$  are 0.53° and 1.17°. These differences can be attributed to the higher rotational flexibility of the biquinoline ligand relative to phenanthroline-based ligands, which have fused ring backbones. The subtle of the unit cell (Figure S23, Figure S24).

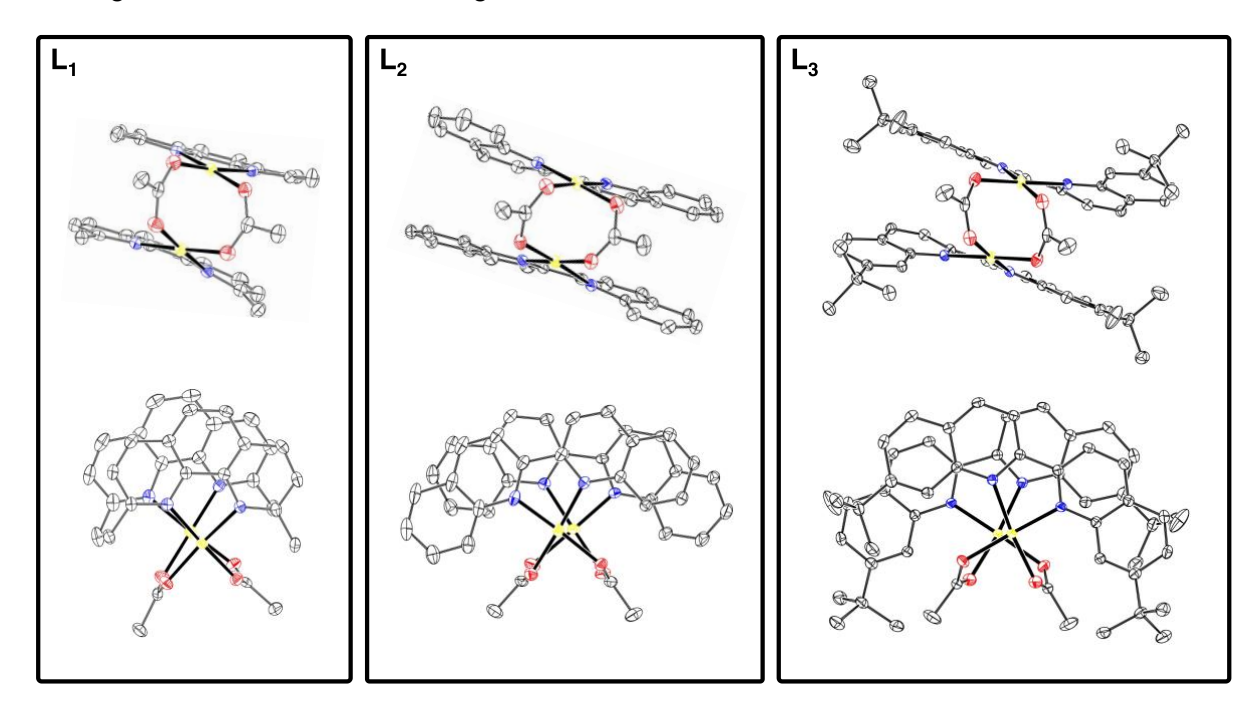


**Figure 9.** Crystal structures of [(L)Pd( $\mu$ -OAc)]<sub>2</sub>[OTf]<sub>2</sub> for L = L<sub>1</sub>, L<sub>2</sub>, and L<sub>3</sub>. ORTEP images for [(L<sub>1</sub>)Pd( $\mu$ -OAc)]<sub>2</sub>[OTf]<sub>2</sub> were generated from the structure originally reported by Conley et al.<sup>17</sup> (CCDC number: 678565). For all structures, ellipsoids are drawn at the 50% probability level and hydrogen atoms and triflate anions are omitted for clarity. For L<sub>2</sub>, only one of the two dimers contained in the asymmetric unit is shown. For L<sub>3</sub>, the asymmetric unit is half of the dimer, so it was expanded to show two asymmetric units (i.e., one complete dimer).

Examination of the crystal structure of  $[(L_3)Pd(\mu-OAc)]_2[OTf]_2$  also reveals several structural differences from the neocuproine-supported  $[(L_1)Pd(\mu-OAc)]_2[OTf]_2$  (Figure 9, Figure S22). The Pd-Pd bond distance in the  $L_3$  dimer is 3.019 Å, greater than the Pd-Pd distance of 2.958 Å in the neocuproine congener. The 7,7'-di-tert-butyl-2,2'-biquinoline ligand is twisted such that the tert-butyl group on one of the quinoline moieties is pointed away from the center of the molecule, presumably to minimize steric crowding between the two ligands in the dimer. This results in a backbone C-C-C-C torsion angle of -10.13° between the two 7-tert-butyl-quinoline halves of the ligand. This backbone torsion is greater than that observed in the crystal structures of both  $[(L_2)Pd(\mu-OAc)]_2[OTf]_2$  and  $[(L_1)Pd(\mu-OAc)]_2[OTf]_2$ .

When viewed along the Pd-Pd axis, the neocuproine ligands in  $[(L_1)Pd(\mu-OAc)]_2[OTf]_2$  nearly overlap. However, moving from  $L_1$  to  $L_2$  to  $L_3$ , the angular offset between the two ligands in the dimer increases; the N-Pd-Pd-N dihedral (same side) has an average absolute value of 9.22° for  $L_1$ , 17.72° for  $L_2$ , and 34.24° for  $L_3$  (Table S5). These differences, among the others discussed above, demonstrate the diversity of ligand structures compatible with alcohol oxidation catalysis within the  $[(L)Pd(\mu-OAc)]_2[OTf]_2$  framework.

## Oxidative lactonization of $\alpha$ , $\omega$ -diols

The oxidative lactonization of  $\alpha,\omega$ -diols (including N-substituted diethanolamines) with  $[(L_1)Pd(\mu-OAc)]_2[OTf]_2$  has proven a useful strategy for the synthesis of lactone and morpholinone monomers for ring-opening polymerization.<sup>20, 47-49</sup> However, the biquinoline complex  $[(L_2)Pd(\mu-OAc)]_2[OTf]_2$  proved inefficient as a catalyst precursor for this class of reactions; the aerobic oxidation of N-Boc diethanolamine produced 36% yield of the lactol intermediate and just 9% of the lactone by NMR (5 mol% Pd, 48 hr, 60°C, 0.1 M in CD<sub>3</sub>CN).

The catalyst derived from the substituted biquinoline  $L_3$  was more effective for synthesis of lactones, affording comparable yields to those obtained with the neocuproine-ligated complex even with 50-75% lower Pd loadings (Figure 10). The aerobic oxidative lactonization of N-Boc diethanolamine in the presence of 2.5 mol% [( $L_3$ )Pd( $\mu$ -OAc)]<sub>2</sub>[OTf]<sub>2</sub> (5 mol% Pd) produces the corresponding N-Boc morpholinone in 87% yield after 16 hours. Under the same conditions, the lactonization of diethylene glycol to form *p*-dioxanone goes to completion (>99% yield by NMR). The lactonization of N-Phenyl diethanolamine with 5 mol% Pd affords N-Phenyl morpholinone in 67% yield in only 3 hours; when the Pd loading is lowered to just 2.5 mol%, a 71% yield of the morpholinone is achieved in 24 hours. In contrast, catalytic oxidation of diethanolamines with the neocuproine complex [( $L_1$ )Pd( $\mu$ -OAc)]<sub>2</sub>[OTf]<sub>2</sub> typically requires approximately 10 mol% Pd and proceeds overnight or over the course of several days at 60°C.<sup>20, 47</sup> Together, these data demonstrate that use of the substituted biquinoline ligand  $L_3$  substantially improves catalyst performance, facilitating synthesis of valuable lactone products.

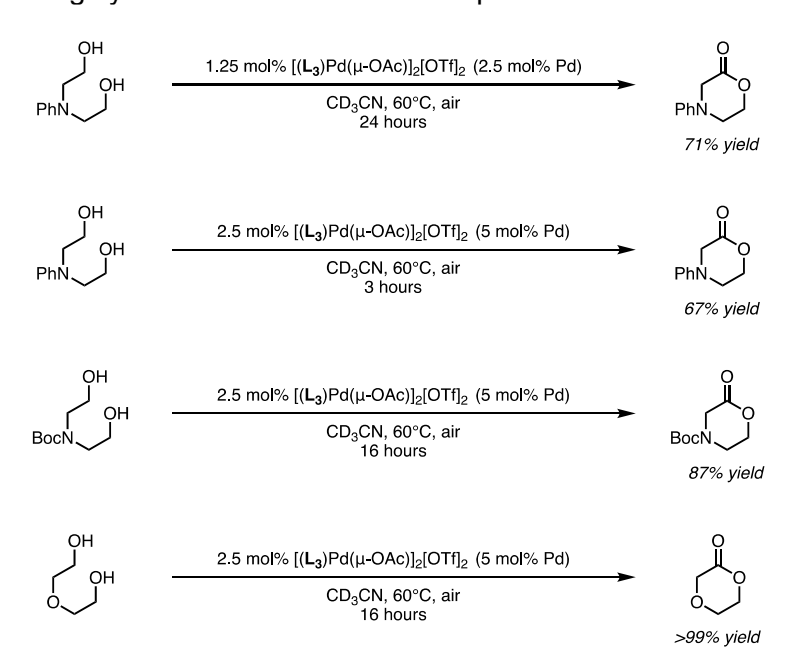


**Figure 10.** Oxidative lactonization of  $\alpha,\omega$ -diols with [(L<sub>3</sub>)Pd( $\mu$ -OAc)]<sub>2</sub>[OTf]<sub>2</sub> (prepared *in situ*). Yields were determined by <sup>1</sup>H NMR.

## Selective oxidation of unprotected glycosides

Biquinoline-supported Pd complexes are also effective for the aerobic oxidation of unprotected carbohydrates. Previous studies have shown that  $[(\mathbf{L_1})\text{Pd}(\mu\text{-OAc})]_2[\text{OTf}]_2$  is selective for the oxidation of certain classes of unprotected alkyl glycosides to 3-ketoses; the minor products of these reactions are the 4-ketoses.<sup>23, 25, 27, 50</sup> Wan and Minnaard et al.<sup>50</sup> recently reported DFT calculations that suggest that the endocyclic oxygen of pyranosides leads to preferential  $\beta$ -hydride elimination at the C3 position with the  $[(\mathbf{L_1})\text{Pd}]^{2+}$  complexes, providing an electronic bias for oxidation at C3.

To probe the relationship between ligand structure and selectivity with this class of complex substrates, we evaluated the reactivity of two model alkyl glycosides: methyl-6-deoxy- $\alpha$ -D-glucopyranoside (**G1**), a C4-OH equatorial glycoside for which the neocuproine-supported catalyst  $[(L_1)Pd(\mu\text{-OAc})]_2[OTf]_2$  exhibits high selectivity for 3C oxidation, and methyl- $\alpha$ -L-fucopyranoside (**G2**), a C4-OH axial glycoside for which oxidation with  $[(L_1)Pd(\mu\text{-OAc})]_2[OTf]_2$  is less selective, yielding approximately equal amounts of the 3- and 4-ketose products.<sup>23</sup>

Under the conditions described in Figure 11A, oxidation of the glycoside **G1** with the neocuproine complex  $[(L_1)Pd(\mu\text{-OAc})]_2[OTf]_2$  affords the 3- and 4-ketoses in yields of 55 and 17%, respectively. The biquinoline complex  $[(L_2)Pd(\mu\text{-OAc})]_2[OTf]_2$  exhibits increased selectivity for formation of the 3-ketose, affording 70% of the 3-ketose product and just 2% of the 4-ketose product as determined by NMR. However, the complex with the more sterically demanding biquinoline ligand  $L_3$  is less selective for this glycoside, affording the 3- and 4-ketoses in similar yields (Figure 11A). The related substrate methyl- $\alpha$ -D-glucopyranoside was also subjected to oxidation with  $L_1$ - and  $L_3$ -supported catalysts; in this case  $[(L_3)Pd(\mu\text{-OAc})]_2[OTf]_2$  was again less selective than  $[(L_1)Pd(\mu\text{-OAc})]_2[OTf]_2$  for C3-OH over C4-OH oxidation, and no other major products (i.e., corresponding to oxidation of the primary C6-OH) were detected in the reaction mixture (Figure S20).



**Figure 11. A:** Oxidation of **G1** (methyl-6-deoxy-α-D-glucopyranoside) with L<sub>1-</sub>, L<sub>2-</sub>, and L<sub>3</sub>-supported catalysts. <sup>†</sup>Standard conditions: 2.5 mol% [(L)Pd(μ-OAc)]<sub>2</sub>[OTf]<sub>2</sub> (5% Pd, catalyst prepared *in situ*), 9:1 CD<sub>3</sub>CN:D2O, 60°C, air, 48 hours. <sup>††</sup>18 hours. **B**: Oxidation of **G2** (methyl-α-L-fucopyranoside) with L<sub>1-</sub>, L<sub>2-</sub>, and L<sub>3</sub>-supported catalysts. <sup>‡</sup>Standard conditions: 2.5 mol% [(L)Pd(μ-OAc)]<sub>2</sub>[OTf]<sub>2</sub> (5% Pd), 9:1 CD<sub>3</sub>CN:D<sub>2</sub>O, 60°C, 3 equiv. 1,4-benzoquinone, air, 6 hours. <sup>‡‡</sup>Entry B1 is reproduced from Chung et al.<sup>23</sup> 1.5 mol% [(L)Pd(μ-OAc)]<sub>2</sub>[OTf]<sub>2</sub> (3% Pd), 10:1 CD<sub>3</sub>CN:D<sub>2</sub>O, 50°C, 1.5 equiv. 1,4-benzoquinone, air, 2 hours. <sup>‡‡</sup>48 hours, catalyst prepared *in situ*. Yields were determined by <sup>1</sup>H NMR.

The selectivity observed for the fucopyranoside G2 is complementary to that observed with the glucopyranoside G1. Complexes bearing  $L_1$  and  $L_2$  both exhibited poor selectivity for the fucopyranoside G2 (Figure 11B, Figure S21), but the complex supported by the substituted

biquinoline ligand  $L_3$  demonstrated high selectivity for G2, affording the 4-ketose in 53% yield and the 3-ketose in 5% yield, which translates to 10:1 selectivity for the 4-ketose over the 3-ketose. Oxidation of glycosides to form 4-ketoses with high selectivity has been reported with an organotin catalyst;<sup>51</sup> however, 4-ketoses are otherwise challenging to access from unprotected carbohydrates. We propose that steric interactions between the bulky  $L_3$  ligand and glycoside substrates may overcome intrinsic electronic factors that favor oxidation at C3.<sup>50</sup> The dependence of chemoselectivity on ligand structure observed here therefore offers an opportunity to obtain rare oxidized glycosides, which can undergo further functionalization to yield valuable carbohydrate products.<sup>29, 52-55</sup>

#### **Preparative-scale oxidations**

Preparative-scale oxidations were performed to assess the synthetic utility of  $[(L_3)Pd(\mu-OAc)]_2[OTf]_2$  for chemoselective aerobic oxidations at low Pd loadings (Figure 12). All of the transformations were performed with air as the terminal oxidant.

**Figure 12.** Preparative scale aerobic oxidations with  $[(L_3)Pd(\mu-OAc)]_2[OTf]_2$ . Yields are of isolated products after purification.

The oxidation of 3-phenyl-1,2-propanediol to the  $\alpha$ -hydroxyketone product was performed in an open Erlenmeyer flask at room temperature with a total Pd loading of 3.5 mol%. Oxidative lactonizations of N-Boc diethanolamine and N-Phenyl diethanolamine were performed on gram scale to furnish the corresponding morpholin-2-one products in good yields. The conditions for these lactonizations represent improvements from previously published procedures with [(L<sub>1</sub>)Pd( $\mu$ -OAc)]<sub>2</sub>[OTf]<sub>2</sub>, which require 3-3.5 times higher Pd loadings or the use of stoichiometric additives.<sup>20, 24, 47</sup>

# Conclusion

Insights into catalyst deactivation mechanisms were leveraged to develop a chemoselective aerobic oxidation catalyst with improved oxidative stability. Previous studies of  $[(L_1)Pd(\mu-OAc)]_2[OTf]_2$  demonstrating the susceptibility of the ligand benzylic  $C(sp^3)$ -H bonds to oxidation informed the choice of the biquinoline ligand  $L_2$ , which completely lacks such bonds and exhibits a more than threefold increase in aerobic TON compared to the neocuproine-ligated catalyst. Subsequent investigations into the slow reaction rates observed with  $L_2$  revealed formation of insoluble multinuclear Pd complexes, an insight which inspired the design of an improved catalyst based on the bulky di-tertbutyl-biquinoline ligand  $L_3$ .  $[(L_3)Pd(\mu-OAc)]_2[OTf]_2$  exhibits rapid.

selective catalysis while retaining the oxidative stability observed with  $[(\mathbf{L_2})Pd(\mu\text{-OAc})]_2[OTf]_2$ , enabling access to useful chemical products with low Pd loadings and simple reaction setups.

Beyond immediate practical impact, the efficacy of  $L_1$ ,  $L_2$ , and  $L_3$ -supported catalysts demonstrates that structurally diverse  $[(L)Pd(\mu-OAc)]_2[OTf]_2$ -type complexes can be compatible with selective oxidation catalysis. As exemplified by the complementary selectivity discovered for the oxidation of alkyl glycoside substrates with  $L_1$ ,  $L_2$ , and  $L_3$ -supported catalysts, exploration of diversified catalyst structures presents opportunities to investigate relationships between catalyst structure, reactivity, and chemoselectivity. Deeper understanding of these relationships may provide insights that facilitate future development of selective and efficient transformations.

# **Supporting Information**

Experimental and theoretical (DFT) procedures, NMR characterization data, mass spectra, X-ray crystallography details, and DFT results with optimized structures

## Acknowledgements

This work was supported by the Department of Energy (Office of Basic Energy Sciences, Catalysis Science Program, Award DE-SC0018168) and the NSF (CHE-2101256). S.R.B. is grateful for a National Science Foundation Graduate Research Fellowship (DGE-1656518). D.P.M and K.C.A thank the Center for Molecular Analysis and Design at Stanford University for graduate research fellowships. T.J.D.C acknowledges the NIH for a fellowship (NIH 1F32GM133150-01). We thank Conor M. Galvin for assistance with modeling disorder in the crystal structure of  $[(\mathbf{L}_2)\text{Pd}(\mu\text{-OAc})]_2[\text{OTf}]_2$ . We thank Laura M. Dornan and Wilson C. Ho for helpful discussions. Part of this work was performed at the Stanford Nano Shared Facilities (SNSF), supported by the National Science Foundation under award ECCS-2026822.

#### References

- 1. Sheldon, R. A.; Arends, I. W. C. E.; ten Brink, G.-J.; Dijksman, A., Green, Catalytic Oxidations of Alcohols. *Accounts of Chemical Research* **2002**, *35* (9), 774-781.
- 2. Gligorich, K. M.; Sigman, M. S., Recent advancements and challenges of palladiumII-catalyzed oxidation reactions with molecular oxygen as the sole oxidant. *Chemical Communications* **2009**, (26), 3854-3867.
- 3. Parmeggiani, C.; Cardona, F., Transition metal based catalysts in the aerobic oxidation of alcohols. *Green Chemistry* **2012**, *14* (3), 547-564.
- 4. Kopylovich, M. N.; Ribeiro, A. P. C.; Alegria, E. C. B. A.; Martins, N. M. R.; Martins, L. M. D. R. S.; Pombeiro, A. J. L., Chapter Three Catalytic Oxidation of Alcohols: Recent Advances. In *Advances in Organometallic Chemistry*, Pérez, P. J., Ed. Academic Press: 2015; Vol. 63, pp 91-174.
- 5. Eisink, N. N. H. M.; Minnaard, A. J.; Witte, M. D., Chemo-and Regioselective Oxidation of Secondary Alcohols in Vicinal Diols. *Synthesis* **2017**, *49* (4), 822-829.
- 6. Wang, D.; Weinstein, A. B.; White, P. B.; Stahl, S. S., Ligand-Promoted Palladium-Catalyzed Aerobic Oxidation Reactions. *Chemical Reviews* **2018**, *118* (5), 2636-2679.
- 7. Urgoitia, G.; Herrero, M. T.; SanMartin, R., CHAPTER 2 Aerobic Oxidation Reactions Using Metal-based Homogeneous Systems. In *Catalytic Aerobic Oxidations*, Mejía, E., Ed. The Royal Society of Chemistry: 2020; pp 16-49.
- 8. Hoover, J. M.; Stahl, S. S., Highly practical copper(I)/TEMPO catalyst system for chemoselective aerobic oxidation of primary alcohols. *Journal of the American Chemical Society* **2011**, *1*33 (42), 16901-16910.
- 9. Dornan, L. M.; Clendenning, G. M. A.; Pitak, M. B.; Coles, S. J.; Muldoon, M. J., N,O-ligated Pd(II) complexes for catalytic alcohol oxidation. *Catalysis Science & Technology* **2014**, *4* (8), 2526-2534.
- 10. Hill, C. K.; Hartwig, J. F., Site-selective oxidation, amination and epimerization reactions of complex polyols enabled by transfer hydrogenation. *Nature Chemistry* **2017**, 9 (12), 1213-1221.
- 11. Bruns, D. L.; Musaev, D. G.; Stahl, S. S., Can Donor Ligands Make Pd(OAc)(2) a Stronger Oxidant? Access to Elusive Palladium(II) Reduction Potentials and Effects of Ancillary Ligands via Palladium(II)/Hydroquinone Redox Equilibria. *Journal of the American Chemical Society* **2020**, *142* (46), 19678-19688.
- 12. Young, I. S.; Baran, P. S., Protecting-group-free synthesis as an opportunity for invention. *Nature Chemistry* **2009**, *1*, 193-205.
- 13. Sheldon, R. A., Fundamentals of green chemistry: efficiency in reaction design. *Chemical Society Reviews* **2012**, *41*, 1437-1451.

- 14. Sheldon, R. A., Catalytic Oxidations in a Bio-Based Economy. *Frontiers in Chemistry* **2020,** 8.
- 15. Hill, C. L.; Weinstock, I. A., On the trail of dioxygen activation. *Nature* **1997**, *388* (6640), 332-333.
- 16. Hill, C. L., Controlled green oxidation. *Nature* **1999**, *401*, 436-437.
- 17. Conley, N. R.; Labios, L. A.; Pearson, D. M.; McCrory, C. C. L.; Waymouth, R. M., Aerobic Alcohol Oxidation with Cationic Palladium Complexes: Insights into Catalyst Design and Decomposition. *Organometallics* **2007**, *26* (23), 5447-5453.
- 18. Painter, R. M.; Pearson, D. M.; Waymouth, R. M., Selective catalytic oxidation of glycerol to dihydroxyacetone. *Angewandte Chemie International Edition* **2010**, *49*, 9456-9459.
- 19. Pearson, D. M.; Conley, N. R.; Waymouth, R. M., Oxidatively Resistant Ligands for Palladium-Catalyzed Aerobic Alcohol Oxidation. *Organometallics* **2011**, *30* (6), 1445-1453.
- 20. Chung, K.; Banik, S. M.; De Crisci, A. G.; Pearson, D. M.; Blake, T. R.; Olsson, J. V.; Ingram, A. J.; Zare, R. N.; Waymouth, R. M., Chemoselective Pd-Catalyzed Oxidation of Polyols: Synthetic Scope and Mechanistic Studies. *Journal of the American Chemical Society* **2013**, *135* (20), 7593-7602.
- 21. Ingram, A. J.; Solis-Ibarra, D.; Zare, R. N.; Waymouth, R. M., Trinuclear Pd3O2 Intermediate in Aerobic Oxidation Catalysis. *Angewandte Chemie International Edition* **2014**, *53*, 5648-5652.
- 22. Ingram, A. J.; Walker, K. L.; Zare, R. N.; Waymouth, R. M., Catalytic Role of Multinuclear Palladium–Oxygen Intermediates in Aerobic Oxidation Followed by Hydrogen Peroxide Disproportionation. *Journal of the American Chemical Society* **2015**, *137* (42), 13632-13646.
- 23. Chung, K.; Waymouth, R. M., Selective Catalytic Oxidation of Unprotected Carbohydrates. *ACS Catalysis* **2016**, *6* (7), 4653-4659.
- 24. Ho, W. C.; Chung, K.; Ingram, A. J.; Waymouth, R. M.; Randall, J. R., Pd-Catalyzed Aerobic Oxidation Reactions: Strategies To Increase Catalyst Lifetimes. *Journal of the American Chemical Society* **2018**, *140* (2), 748-757.
- 25. Jäger, M.; Hartmann, M.; De Vries, J. G.; Minnaard, A. J., Catalytic Regioselective Oxidation of Glycosides. *Angewandte Chemie International Edition* **2013**, *52*, 7809-7812.
- 26. Eisink, N. N. H. M.; Lohse, J.; Witte, M. D.; Minnaard, A. J., Regioselective oxidation of unprotected 1,4 linked glucans. *Organic & Biomolecular Chemistry* **2016**, *14* (21), 4859-4864.
- 27. Eisink, N. N. H. M.; Witte, M. D.; Minnaard, A. J., Regioselective Carbohydrate Oxidations: A Nuclear Magnetic Resonance (NMR) Study on Selectivity, Rate, and Side-Product Formation. *ACS Catalysis* **2017**, *7* (2), 1438-1445.
- 28. Zhang, J.; Eisink, N. N. H. M.; Witte, M. D.; Minnaard, A. J., Regioselective Manipulation of GlcNAc Provides Allosamine, Lividosamine, and Related Compounds. *The Journal of Organic Chemistry* **2019**, *84* (2), 516-525.

- 29. Xiao, G.; Su, G.; Slawin, A. M. Z.; Westwood, N., From Biomass to the Karrikins via Selective Catalytic Oxidation of Hemicellulose-Derived Butyl Xylosides and Glucosides. *European Journal of Organic Chemistry* **2022**, *2022* (15), e202101308.
- 30. Dimakos, V.; Taylor, M. S., Site-Selective Functionalization of Hydroxyl Groups in Carbohydrate Derivatives. *Chemical Reviews* **2018**, *118* (23), 11457-11517.
- 31. Shang, W.; He, B.; Niu, D., Ligand-controlled, transition-metal catalyzed site-selective modification of glycosides. *Carbohydrate Research* **2019**, *474*, 16-33.
- 32. Armenise, N.; Tahiri, N.; Eisink, N. N. H. M.; Denis, M.; Jä, M.; De Vries, J. G.; Witte, M. D.; Minnaard, A. J., Deuteration enhances catalyst lifetime in palladium-catalysed alcohol oxidation. *Chemical Communications* **2016**, *52*, 2189-2191.
- 33. ten Brink, G. J.; Arends, I. W. C. E.; Sheldon, R. A., Green, Catalytic Oxidation of Alcohols in Water. *Science* **2000**, *287* (5458), 1636-1639.
- 34. Buffin, B. P.; Belitz, N. L.; Verbeke, S. L., Electronic, steric, and temperature effects in the Pd(II)-biquinoline catalyzed aerobic oxidation of benzylic alcohols in water. *Journal of Molecular Catalysis a-Chemical* **2008**, *284* (1-2), 149-154.
- 35. Buffin, B. P.; Clarkson, J. P.; Belitz, N. L.; Kundu, A., Pd(II)-biquinoline catalyzed aerobic oxidation of alcohols in water. *Journal of Molecular Catalysis a-Chemical* **2005**, *225* (1), 111-116.
- 36. Selectivity is calculated as %yield(hydroxyacetone)/%conversion(1,2-propanediol).
- 37. Vikse, K. L.; Ahmadi, Z.; Scott McIndoe, J., The application of electrospray ionization mass spectrometry to homogeneous catalysis. *Coordination Chemistry Reviews* **2014**, 279, 96-114.
- 38. Walker, K. L.; Dornan, L. M.; Zare, R. N.; Waymouth, R. M.; Muldoon, M. J., Mechanism of Catalytic Oxidation of Styrenes with Hydrogen Peroxide in the Presence of Cationic Palladium(II) Complexes. *Journal of the American Chemical Society* **2017**, *139* (36), 12495-12503.
- 39. Frisch, M. J.; Trucks, G. W.; Schlegel, H. B.; Scuseria, G. E.; Robb, M. A.; Cheeseman, J. R.; Scalmani, G.; Barone, V.; Petersson, G. A.; Nakatsuji, H.; Li, X.; Caricato, M.; Marenich, A. V.; Bloino, J.; Janesko, B. G.; Gomperts, R.; Mennucci, B.; Hratchian, H. P.; Ortiz, J. V.; Izmaylov, A. F.; Sonnenberg, J. L.; Williams; Ding, F.; Lipparini, F.; Egidi, F.; Goings, J.; Peng, B.; Petrone, A.; Henderson, T.; Ranasinghe, D.; Zakrzewski, V. G.; Gao, J.; Rega, N.; Zheng, G.; Liang, W.; Hada, M.; Ehara, M.; Toyota, K.; Fukuda, R.; Hasegawa, J.; Ishida, M.; Nakajima, T.; Honda, Y.; Kitao, O.; Nakai, H.; Vreven, T.; Throssell, K.; Montgomery Jr., J. A.; Peralta, J. E.; Ogliaro, F.; Bearpark, M. J.; Heyd, J. J.; Brothers, E. N.; Kudin, K. N.; Staroverov, V. N.; Keith, T. A.; Kobayashi, R.; Normand, J.; Raghavachari, K.; Rendell, A. P.; Burant, J. C.; Iyengar, S. S.; Tomasi, J.; Cossi, M.; Millam, J. M.; Klene, M.; Adamo, C.; Cammi, R.; Ochterski, J. W.; Martin, R. L.; Morokuma, K.; Farkas, O.; Foresman, J. B.; Fox, D. J. *Gaussian 16 Rev. A.03*, Wallingford, CT, 2016.
- 40. Lee, C.; Yang, W.; Parr, R. G., Development of the Colle-Salvetti correlation-energy formula into a functional of the electron density. *Physical Review B* **1988**, *37* (2), 785-789.

- 41. Becke, A. D., Density-functional thermochemistry. III. The role of exact exchange. *The Journal of Chemical Physics* **1993**, *98* (7), 5648-5652.
- 42. Ditchfield, R.; Hehre, W. J.; Pople, J. A., Self-Consistent Molecular-Orbital Methods. IX. An Extended Gaussian-Type Basis for Molecular-Orbital Studies of Organic Molecules. *The Journal of Chemical Physics* **1971**, *54* (2), 724-728.
- 43. Hehre, W. J.; Ditchfield, R.; Pople, J. A., Self—Consistent Molecular Orbital Methods. XII. Further Extensions of Gaussian—Type Basis Sets for Use in Molecular Orbital Studies of Organic Molecules. *The Journal of Chemical Physics* **1972**, *56* (5), 2257-2261.
- 44. Hariharan, P. C.; Pople, J. A., The influence of polarization functions on molecular orbital hydrogenation energies. *Theoretica Chimica Acta* **1973**, *28* (3), 213-222.
- 45. Hay, P. J.; Wadt, W. R., Ab initio effective core potentials for molecular calculations. Potentials for K to Au including the outermost core orbitals. *The Journal of Chemical Physics* **1985**, *82* (1), 299-310.
- 46. Ma, W.; Zhang, J.; Xu, C.; Chen, F.; He, Y.-M.; Fan, Q.-H., Highly Enantioselective Direct Synthesis of Endocyclic Vicinal Diamines through Chiral Ru(diamine)-Catalyzed Hydrogenation of 2,2'-Bisquinoline Derivatives. *Angewandte Chemie International Edition* **2016**, *55* (41), 12891-12894.
- 47. Blake, T. R.; Waymouth, R. M., Organocatalytic Ring-Opening Polymerization of Morpholinones: New Strategies to Functionalized Polyesters. *Journal of the American Chemical Society* **2014**, *136* (26), 9252-9255.
- 48. Nicklaus, C. M.; Phua, P. H.; Buntara, T.; Noel, S.; Heeres, H. J.; de Vries, J. G., Ruthenium/1,1'-Bis(diphenylphosphino)ferrocene-Catalysed Oppenauer Oxidation of Alcohols and Lactonisation of α,ω-Diols using Methyl Isobutyl Ketone as Oxidant. *Advanced Synthesis* & *Catalysis* **2013**, *355* (14-15), 2839-2844.
- 49. Xie, X.; Stahl, S. S., Efficient and Selective Cu/Nitroxyl-Catalyzed Methods for Aerobic Oxidative Lactonization of Diols. *Journal of the American Chemical Society* **2015**, *137* (11), 3767-3770.
- 50. Wan, I. C.; Hamlin, T. A.; Eisink, N. N. H. M.; Marinus, N.; de Boer, C.; Vis, C. A.; Codée, J. D. C.; Witte, M. D.; Minnaard, A. J.; Bickelhaupt, F. M., On the Origin of Regioselectivity in Palladium-Catalyzed Oxidation of Glucosides. *European Journal of Organic Chemistry* **2021**, *2021* (4), 632-636.
- 51. Muramatsu, W., Catalytic and Regioselective Oxidation of Carbohydrates To Synthesize Keto-Sugars under Mild Conditions. *Organic Letters* **2014**, *16* (18), 4846-4849.
- 52. Marinus, N.; Tahiri, N.; Duca, M.; Mouthaan, L. M. C. M.; Bianca, S.; van den Noort, M.; Poolman, B.; Witte, M. D.; Minnaard, A. J., Stereoselective Protection-Free Modification of 3-Keto-saccharides. *Organic Letters* **2020**, *22* (14), 5622-5626.
- 53. Bastian, A. A.; Bastian, M.; Jager, M.; Loznik, M.; Warszawik, E. M.; Yang, X.; Tahiri, N.; Fodran, P.; Witte, M. D.; Thoma, A.; Kohler, J.; Minnaard, A. J.; Herrmann, A., Late-Stage

- Modification of Aminoglycoside Antibiotics Overcomes Bacterial Resistance Mediated by APH(3') Kinases. *Chemistry* **2022**, *28* (36), e202200883.
- 54. Reintjens, N. R. M.; Yakovlieva, L.; Marinus, N.; Hekelaar, J.; Nuti, F.; Papini, A. M.; Witte, M. D.; Minnaard, A. J.; Walvoort, M. T. C., Palladium-Catalyzed Oxidation of Glucose in Glycopeptides. *European Journal of Organic Chemistry* **2022**, *2022* (25), 7.
- 55. Zhang, J.; Reintjens, N. R. M.; Dhineshkumar, J.; Witte, M. D.; Minnaard, A. J., Site-Selective Dehydroxy-Chlorination of Secondary Alcohols in Unprotected Glycosides. *Organic Letters* **2022**, *24* (29), 5339-5344.